DR JOSÉ MANUEL ESTEVEZ (Orcid ID : 0000-0001-6332-7738)

Article type : Rapid Report

*Rapid report*

# A cell surface arabinogalactan-peptide influences root hair cell fate

Cecilia Borassi[1,#], Javier Gloazzo Dorosz[1,#,*], Martiniano M. Ricardi[2,#], Mariana Carignani Sardoy[1], Laercio Pol Fachin[3], Eliana Marzol[1], Silvina Mangano[1], Diana Rosa Rodríguez Garcia[1], Javier Martínez Pacheco[1], Yossmayer del Carmen Rondón Guerrero[1], Silvia M. Velasquez[1,**], Bianca Villavicencio[4], Marina Ciancia[5], Georg Seifert[6], Hugo Verli[4] & José M. Estevez[1,7,†]

[1]Fundación Instituto Leloir, Av. Patricias Argentinas 435, Buenos Aires CP C1405BWE, Argentina.

[2]Instituto de Fisiología, Biología Molecular y Neurociencias (IFIByNE-CONICET), Departamento de Fisiología y Biología Molecular y Celular (FBMC), Facultad de Ciencias Exactas y Naturales, Universidad de Buenos Aires C1428EGA, Argentina.

[3]Centro Universitário CESMAC, Maceió, 57051160, Brazil.

[4]Centro de Biotecnologia, Universidade Federal do Rio Grande do Sul CP 15005, Porto Alegre 91500-970 RS, Brazil.

[5]Universidad de Buenos Aires, Facultad de Agronomía, Departamento de Biología Aplicada y Alimentos, Cátedra de Química de Biomoléculas, Buenos Aires, Argentina and CONICET-Universidad de Buenos Aires, Centro de Investigación de Hidratos de Carbono (CIHIDECAR), C1428EGA, Buenos Aires, Argentina.

[6]University of Natural Resources and Life Science, BOKU Vienna, Department of Applied Genetics and Cell Biology, Muthgasse 11 A-1190, Vienna, Austria.

[7]Centro de Biotecnología Vegetal (CBV), Facultad de Ciencias de la Vida, Universidad Andrés Bello Santiago, 8370186, Chile and Millennium Institute for Integrative Biology (iBio), Santiago, 8331150, Chile.

[#]co-first authors

[†]Correspondence should be addressed. Email: jestevez@leloir.org.ar; Tel: +541152387500 EXT. 3206. ORCID 0000-0001-6332-7738.

Received: *4 December 2020*

Accepted: *12 February 2020*

**Summary**

- **Root hairs (RHs) develop from specialized epidermal trichoblast cells, whereas epidermal cells that lack RHs are known as atrichoblasts. The mechanism controlling RH cell fate is only partially understood.**

- **RH cell fate is regulated by a transcription factor complex that promotes the expression of the homeodomain protein GLABRA 2 (GL2), which blocks RH development by inhibiting ROOT HAIR DEFECTIVE 6 (RHD6). Suppression of GL2 expression activates RHD6, a series of downstream TFs including ROOT HAIR DEFECTIVE 6 LIKE-4 (RSL4) and their target genes, and causes epidermal cells to develop into RHs. Brassinosteroids (BRs) influence RH cell fate. In the absence of BRs, phosphorylated BIN2 (a Type-II GSK3-like kinase) inhibits a protein complex that regulates GL2 expression.**

- **Perturbation of the arabinogalactan peptide AGP21 in *Arabidopsis thaliana* triggers aberrant RH development, similar to that observed in plants with defective BR signaling. We reveal that an *O*-glycosylated AGP21 peptide, which is positively regulated by BZR1, a transcription factor activated by BR signaling, affects RH cell fate by altering *GL2* expression in a BIN2-dependent manner.**

- **Changes in cell surface AGP disrupts BR responses and inhibits the downstream effect of BIN2 on the RH repressor GL2 in root epidermis.**

Key words: *Arabidopsis thaliana*, root hair cell fate, Arabinogalactan peptide 21, Brassinosteroids, *O*-glycosylation

**Introduction**

Plant roots not only anchor the plant into the soil but also allow them to absorb water and nutrients from the soil. Root hairs (RHs) are single cell protrusions developed from the epidermis that increase the root surface area exposed to the soil enhancing water and nutrients uptake. Many factors determine whether, or not, an epidermal cell will develop into a RH. These factors include both, environmental cues (such as nutrients in the soil) and signals from the plant itself, such as hormones like brassinosteroids (BRs), ABA, ethylene and auxin (Van Hengel et al. 2004; Masucci and Schiefelbein 1994, 1996; Kuppusamy et al., 2009). RH cell fate in the model plant *Arabidopsis* is controlled by a well-known developmental program, regulated by a complex of transcription factors composed by WEREWOLF (WER)-GLABRA3 (GL3)/ENHANCER OF GLABRA3 (EGL3)-TRANSPARENT GLABRA1 (TTG1) that promotes the expression of the homeodomain protein GLABRA 2 (GL2) (Ryu et al. 2005; Song et al. 2011; Schiefelbein et al. 2014; Balcerowicz et al. 2015), which ultimately blocks the root hair pathway by inhibiting ROOT HAIR DEFECTIVE 6 (RHD6) (Lin et al. 2015). The suppression of GL2 expression triggers epidermal cells to enter into the root hair cell fate program by the concomitant activation of RHD6 and a well-defined downstream gene network. As a consequence, RH and non-RH cell files are patterned alternately in rows within the root epidermis. In trichoblasts, a second transcription factor complex composed by CAPRICE (CPC)-GL3/EGL3-TTG1 suppresses GL2 expression (Schiefelbein et al. 2014), forcing cells to enter the RH cell fate program via concomitant RHD6 activation and downstream TFs, including RSL4, and RH genes (Yi et al. 2010). The plant steroid hormones, BRs play essential roles in regulating many developmental processes (Savaldi-Goldstein et al., 2007; 2010; Hacham et al., 2011; Yang et al., 2011). BRs are perceived by the receptor kinase BRASSINOSTEROID INSENSITIVE 1 (BRI1) (Li & Chory, 1997; Hothorn et al., 2011; She et al., 2011). One of the BRI1 substrate, BR-SIGNALING KINASE (BSK), transduces the BR signaling through *bri1* SUPPRESSOR 1 (BSU1) to inactivate a GSK3-like kinase BRASSINOSTEROID INSENSITIVE 2 (BIN2), which triggers high levels of the dephosphorylated form of transcriptional factors BRI1 EMS SUPPRESSOR 1 (BES1)/BRASSINAZOLE RESISTANT 1 (BZR1) in the nucleus to regulate gene expression (Yan et al. 2009; Yang et al., 2011). In recent years, a molecular mechanism was proposed by which BR signaling controls RH cell fate by inhibiting BIN2 phosphorylation activity to positively modulate *GL2* expression thus hindering the RH development in trichoblast cells and

promoting the lack of RHs in the root epidermis (Chen et al. 2014). On the contrary, phosphorylated BIN2 under the absence/low amounts of BRs, is able to phosphorylate TTG1, controlling protein complex TTG1-WER-GL3/EGL3 activity and repressing *GL2* expression to promote anomalous RH development in atrichoblast cells (Chen et al. 2014). The later scenario produces contiguous RH in the root epidermis that is unusual in Wt Col-0 roots.

Plant cell surface proteoglycans known as arabinogalactan proteins (AGPs) function in a broad developmental processes such as cell proliferation, cell expansion, organ extension, and somatic embryogenesis (Tan et al. 2004; Seifert & Roberts 2007; Pereira et al. 2015; Ma et al. 2018). The precise mechanisms underlying AGP action in these multiple processes are completely unknown (Ma et al. 2018). AGP peptides are post-translationally modified in the ER-Golgi, undergoing signal peptide (SP) removal, proline-hydroxylation/Hyp-*O*-glycosylation, and C-terminal GPI anchor signal (GPI-AS) addition (Schultz et al. 2004; Ma et al. 2018). Processed mature AGP-peptides are 10–13 amino acids long and bear few putative *O*-glycosylation sites (*O*-AG). Few prolines in the AGP peptides are hydroxylated *in vivo* as Hyp (Hyp=O), suggesting that AGP peptides are *O*-glycosylated at maturity (Schultz et al. 2004). All these posttranslational modifications make the study of AGPs very complex with almost no defined biological functions for any individual AGP (Ma et al. 2018). Interestedly, in this work we have identified that disruption of plant specific AGPs, and in particular of a single *O*-glycosylated AGP peptide (AGP21), interfere in a specific manner with BR responses and BIN2-downstream effect on the repression of RH development. We have found that the absence of an *O*-glycosylated AGP21-peptide, positively regulated by the BR transcription factor BZR1, impacts on RH cell fate in a BIN2-dependent manner by controlling in a negative manner the GL2 expression and enhancing the expression of the downstream RH specific genes *RHD6*, *RSL4*, and *EXP7*.

## Materials and Methods

**Growth conditions.** All plant materials used in this study were in the Columbia-0 ecotype background of *Arabidopsis thaliana*. Seeds were sterilized and placed on half-strength (0.5X) Murashige and Skoog (MS) medium (Sigma-Aldrich) pH 5.8 supplemented with 0.8% agar. For root measurements, RNA extraction and confocal microscopy 7-day old seedlings were grown on square plates placed vertically at 22°C with continuous light, after stratification in dark at 4°C for 5 days on the plates. Seedlings on plates were transferred to soil and kept in the greenhouse in long-day conditions to obtain mature plants for transformation, genetic crossing, and amplification of seeds.

**Plant material.** For identification of homozygous T-DNA knockout lines, genomic DNA was extracted from rosette leaves. Confirmation by PCR of a unique band corresponding to T-DNA insertion in the target genes AGP15 (At5G11740: SALK_114736), AGP21 (At1G55330: SALK_140206), HPGT1-HPGT3 (AT5G53340: SALK_007547, AT4G32120: SALK_070368, AT2G25300: SALK_ 009405) GALT29A (At1G08280: SALK_030326; SALK_113255; SAIL_1259_C01) and RAY1 (At1G70630: SALK_053158) were performed using an insertion-specific LBb1.3 for SALK lines or Lb1 for SAIL lines. Primers used are listed in **Table S1**. The stable transgenic lines used in this study are summarized in **Table S2**.

**Pharmacological treatments.** ethyl-3,4-dihydrohydroxybenzoate (EDHB) and $\alpha,\alpha$-Bipyridyl (DP) D216305 SIGMA-ALDRICH were used as P4Hs inhibitors. DP chelates the cofactor $Fe^{2+}$ [9] and the EDHB interacts with the oxoglutarate-binding site of P4Hs (Majamaa et al. 1986). Specific Yariv phenylglycoside (for 1,3,5-tri-(p-glycosyloxyphenylazo)-2,4,6-trihydroxybenzene), β-glucosyl Yariv phenylglycoside (β-Glc-Yariv) was used for AGP-depletion (Kitazawa et al.2013). α-mannosyl Yariv phenylglycoside (α-Man-Yariv) was used as negative control for phenylglycoside treatment. Both, β-Glc-Y and $\alpha$-Man-Y are Yariv-phenylglycosides and its specificity for AGPs relies on the β-configuration of the glycosyl residues attached to the phenylazotrihydroxybenzene core (Yariv et al. 1967). DP, EDHB, or Yariv reagents were added to MS media when MS plates were made.

Seedlings were grown for 4 days in MS 0.5X media and then transferred for 3 days more to MS 0.5X plates with DP, EDHB, or Yariv reagents at the concentration indicated.

**Quantification of RH cell fate.** In order to determine the RH patterning, images of root tips were taken using an Olympus stereomicroscope at maximum magnification (50X). The presence of contiguous RH was analyzed using ImageJ, starting from the differentiation zone to the elongation zone. The amount of contiguous RH was expressed as a percentage of total RH for rectangular root areas of 200 µm in width x 2mm in length (n=20) with three biological replicates. Quantitative and statistical analysis was carried on using GraphPad software. To analyze the alteration in RH cell fate, root cell walls of reporter lines were stained with 5 µg/ml propidium iodide and confocal microscopy images were taken using a Zeiss LSM 710 Pascal microscope, 40X objective N/A= 1.2.

**Root hair density measurements.** RH density was determined as the number of root hairs in 1 $mm^2$ segments of root epidermis from 7 day old seedlings. Images of root were taken using an Olympus stereomicroscope at maximum magnification (50X). At least six plants were measured for each genotype, and each experiment was replicated three times. Correlation analysis was performed to determine the relationship between the percentage of contiguous RH % and RH density per genotype.

**AGP21 variants.** AGP21 promoter region (AGP21p) comprising 1,5 Kbp upstream of +1 site was amplified by PCR and cloned into pGWB4 to obtain AGP21p::GFP construct. Synthetic DNA was designed containing full length AGP21 cDNA and Venus fluorescent protein cDNA between AGP21 signal sequence and the mature polypeptide (Venus-AGP21), containing GatewayTM (Life Technologies) attB1 and attB2 sites. Recombinase-mediated integration of the PCR fragment was made into pEntry4Dual. pEntry4Dual/Venus-AGP21 construction was recombined into the vector pGWB2 (Invitrogen, Hygromicyn R) in order to overexpress Venus-AGP21 under 35S mosaic virus promoter (35S::Venus-AGP21). Also, Venus-AGP21 construct was cloned into pGWB1 (no promoter, no tag) and AGP21p was sub-cloned in the resulting vector to express AGP21 reporter under the control of its endogenous promoter (AGp21::Venus-AGP21). Wild type and T-DNA

*agp21* mutant plants were transformed by using Agrobacterium (strain GV3101+pSoup). Plants were selected with hygromycin (30 µg/ml) and several independent transgenic plants were isolated for each construct. At least three homozygous independent transgenic lines of Col-0/AGP21::GFP, *agp21*/AGP21::Venus-AGP21 and *agp21*/35S::AGP21-GFP were obtained and characterized.

**Gene expression analysis**. For RT-PCR analysis, total RNA was isolated from roots of 7-day-old seedlings using RNeasy Plant Mini Kit (Qiagen) according to the manufacturer's instructions. cDNA synthesis was achieved using M-MLV reverse transcriptase (Promega). PCR reactions were performed in a T-ADVANCED S96G (Biometra) using the following amplification program: 4 min at 95°C, followed by 35 cycles of 20 secs at 95°C, 30 secs at 57°C and 30 secs at 72°C. RT-PCR was performed to assess AGP15 and AGP21 transcript levels in wild type and T-DNA mutant *agp15* and *agp21*. PP2A was used as an internal standard. All primers used are listed in **Table S1.**

**Confocal microscopy.** Confocal laser scanning microscopy was performed using Zeiss LSM 510 Meta and Zeiss LSM 710 Pascal. Fluorescence was analyzed by using laser lines of 488 nm for GFP or 514 nm for YFP excitation, and emitted fluorescence was recorded between 490 and 525 nm for GFP and between 530 and 600 nm for YFP (40X objective, N/A= 1.2). Z series was done with an optical slice of 1 µm. Fluorescence intensities were summed for quantification along a segmented line comprising both in trichoblast and atrichoblast cell layers (starting at the meristematic zone towards the differentiation zone). For the quantification of fluorescence corresponding to Venus-AGP21 in control roots and roots treated with β-Glc-Y or with BL, the plot profile command in Image J was used, 5 replicates for each root (n=5) were observed. Statistical analysis was performed using GraphPad (version 5). In a similar manner, to quantify the levels of expression of *AGP21::V-AGP21* in trichoblast and atrichoblast cell layers in the root meristematic zone, a plot profile line of 100 µm in length from the root tip to the expansion zone was recorded in Image J and 5 replicates for each root (n=5) were observed.

**AGP21 Immunoblotting detection.** Proteins were extracted from roots of 7-day-old seedlings using extraction buffer (20mM TRIS-HCl pH8.8, 150mM NaCl, 1mM EDTA, 20% glycerol, 1mM

PMSF, 1X protease inhibitor Complete® Roche) at 4°C. After centrifugation at 21.000*g* at 4ºC for 20min, protein concentration in the supernatant was measured and equal protein amounts were loaded onto a 6% SDS- PAGE gel. Proteins were separated by electrophoresis and transferred to nitrocellulose membranes. Anti-GFP mouse IgG (Roche Applied Science) was used at a dilution of 1:1.000 and it was visualized by incubation with goat anti-mouse IgG secondary antibodies conjugated to horseradish peroxidase (1:10.000) followed by a chemiluminescence reaction (Clarity ™ Western ECL Substrate, BIO-RAD).

**Transient expression assays in *Nicotiana benthamiana*.** To test the sub-cellular localization of AGP21, 5-day-old *N. benthamiana* leaves were infiltrated with *Agrobacterium* strains (GV3101) carrying 35S::Venus-AGP21 and BAK1-RFP constructs. After 2 days, images of the lower leaf epidermal cells were taken using a confocal microscope (LSM5 Pascal) to analyze Venus-AGP21 expression. Plasmolysis was done using 800 mM mannitol.

**Molecular dynamics (MD) simulations.** MD simulations were performed on two non-glycosylated and seven glycosylated Ala1-Pro2-Ala3-Pro4-Ser5-Pro6-Thr7-Ser8 (APAPSPTS) peptides, in which the starting structure was constructed as a type-II polyproline helix, with $\phi \sim -75$ and $\psi \sim 145$. The non-glycosylated motifs differ by the presence of alanine (AAAASATS), proline (APAPSPTS) or 4-*trans*-hydroxyproline (AOAOSOTS) residues. At the same time, the glycosylated motifs reflect different peptide glycoforms, constructed as full glycosylated (AOAOSOTS). Every *O*-glycosylation site was filled with an arabinogalactan oligosaccharide moiety (**Fig. S6b**), in which the *O*-glycan chains and carbohydrate-amino acid connections were constructed based on the most prevalent geometries obtained from solution MD simulations of their respective disaccharides, as previously described (Pol-Fachin & Verli 2012), thus generating the initial coordinates for glycopeptide MD calculations. Such structures were then solvated in rectangular boxes using periodic boundary conditions and the SPC water model (Berendsen et al. 1984). Both carbohydrate and peptide moieties were described under GROMOS96 43a1 force field parameters, and all MD simulations and analyses were performed with GROMACS simulation suite, version 4.5.4 (Hess et al. 2008). The Lincs method (Hess et al. 1997) was applied to constrain covalent bond lengths, allowing an integration step of 2 fs after an initial energy

minimization using the Steepest Descents algorithm. Electrostatic interactions were calculated with the generalized reaction-field method Tironi et al. (1995). Temperature and pressure were kept constant at 310 K and 1.0 atom, respectively, by coupling (glyco)peptides and solvent to external baths under V-rescale thermostat Bussi et al. 2007) and Berendsen barostat (Berendsen et al. 1987) with coupling constants of $t$ =0.1 and $t$=0.5, respectively, via isotropic coordinate scaling. The systems were heated slowly from 50 to 310 K, in steps of 5 ps, each one increasing the reference temperature by 50 K. After this thermalization, all simulations were further extended to 100 ns. See **Table S3**.

## Results and Discussion

### AGP perturbation influences root hair (RH) cell fate programming

To determine whether *O*-glycosylated AGPs regulate specific RH developmental processes, we exposed roots of *Arabidopsis thaliana* to β-glucosyl Yariv (β-Glc-Y), which specifically binds structures in the *O*-glycans of AGPs: oligosaccharides with at least 5–7 units of 3-linked *O*-galactoses (Yariv et al. 1967; Kitazawa et al. 2013). β-Glc-Y–linked AGP complexes on the cell surface induce AGP aggregation and disrupt native protein distribution, triggering developmental reprogramming (Guan & Nothnagel 2004; Sardar et al. 2006). α-mannosyl Yariv (α-Man-Y), an analogue that does not bind to AGPs, served as the control. While α-Man-Y treatment did not affect RH cell fate (≈2–5% of total RHs that are contiguous in a similar range present in Wt Col-0), β-Glc-Y treatment increased contiguous RH development (≈30-35%) (**Figure S1a**), suggesting that *O*-glycosylated AGPs may influence RH cell fate.

To test whether *O*-glycans on hydroxyproline-rich glycoproteins (HRGPs) alter RH cell fate, we blocked proline 4-hydroxylase enzymes (P4Hs) that catalyse proline (Pro)-hydroxylation into hydroxyl-proline units (Hyp), the subsequent step of HRGP *O*-glycosylation (Velasquez et al. 2011, 2015a). Two P4H inhibitors, α,α-dipyridyl (DP) and ethyl-3,4-dihydroxybenzoate (EDHB), prevent Pro-hydroxylation (Barnett 1970; Majamaa et al. 1986); both increased contiguous RH development to ≈15–20% (**Figure S1b**). Additionally, *p4h5* (a key P4H in roots [Velasquez et al. 2011; 2015a]) and four glycosyltransferase (GT) mutants defective in AGP and related proteins *O*-glycosylation (*hpgt* triple mutant*; ray1*, *galt29A*, and *fut4 fut6*) (see **Table S4**) showed significantly increased (≈8–20%) ectopic RH development (**Figure 1a**), sustaining the previous report that the triple mutant *hpgt* mutant has an increased RH density (Ogawa-Ohnishi & Matsubayashi 2015). These mutants were mostly insensitive to β-Glc-Y; however, the treatment increased the number of contiguous RHs in *fut4 fut6,* although to a lesser extent than in the wild type (**Figure 1b**). This minor effect is expected since *O*-fucosylation in AGPs occurs at low levels in roots (Trypona et al. 2014). β-Glc-Y inhibits root cell expansion (Willats & Knox 1996; Ding & Zhu 1997). On the contrary, glycosyltransferase (GT) mutations affecting extensin (EXTs) and related proteins *O*-glycosylation (e.g. *rra3* and *sgt1 rra3*; **Table S4**) drastically affect only RH cell

elongation (Velasquez et al. 2015b). These mutations did not affect RH cell fate, and β-Glc-Y stimulated ectopic RH development as in Wt Col-0, indicating that EXT *O*-glycosylation might not function in RH cell fate reprogramming (**Table S4**, **Figure 1c**), and specifically *O*-glycans attached to AGPs and related glycoproteins do*. P4H5* and *AGP-related GTs (e.g. RAY1, GALT29A, HPGT1-HPGT3* and *FUT4/FUT6),* are expressed in the root epidermis elongation and differentiation zones (**Figure S2**)*.* Under-arabinosylated AGPs in *ray1* and, to a lower extent, under–*O*-fucosylated AGPs in *fut4 fut6* show root growth inhibition (Liang et al. 2013; Trypona et al. 2014), highlighting a key role for AGP *O*-glycans in regulating root growth, albeit by unknown mechanisms. Our results using DP/EDHB and β-Glc-Y treatments as well as mutants in the AGPs *O*-glycosylation pathway suggest that AGPs and related proteins might be involved in RH cell fate.

**The AG peptide AGP21 influences RH cell fate**

Brassinosteroid (BR) signaling regulates RH cell patterning (Cheng et al. 2015). The BR-insensitive mutant, *bri1-116*, and *bak1* developed many (≈20%-25%) contiguous RH cells (**Figure S3a**), resembling plants subjected to β-Glc-Y and DP/EDHB treatments (**Figure S1**). *p4h5*, *hpgt* triple mutant*, ray1-1*, *galt29A*, and *fut4 fut6* mutants exhibited similar phenotypes, suggesting that an interplay between cell surface AGPs and BR signaling may determine RH cell fate. Chromatin-immunoprecipitation (ChIP)-sequencing and RNA-sequencing indicated that BZR1 directly upregulates few *AGPs* gene expression, most predominantly *AGP21* (Sun et al. 2010). Based on this, we decided to investigate how root epidermal BR signalling regulates *AGP21* expression. Since the *AGP21* regulatory region contains one BZR1 binding motif (E-BOX, CATGTG at -279 bp relative to ATG start codon), we tested whether BR directly modulates *AGP21* expression. Compared with no treatment, 100 nM BL (brassinolide, BR's most active form) enhanced of both AGP21p::GFP (transcriptional reporter) and AGP21p::V-AGP21 (V= Venus tag; translational reporter) expression (**Figure S3b–c**). Expression of *AGP21p::GFP* in *bri1-116* resulted in lower *AGP21* signal than in untreated wild type (**Figure S3b**), confirming that BR-mediated BZR1 controls *AGP21* expression in the root. To visualize if drastic changes are induced under β-Glc-Y—treatment on epidermis cells and AGPs, we decided to analyse the localization of AGP21p::V-AGP21 in this condition. Treatment with β-Glc-Y—but not α-Man-Y—resulted in a clear accumulation of AGP21p::Venus-AGP21 protein at transverse cell walls in the root epidermis

(**Figure S1c**), thus confirming the expected effect on aggregating AGPs at the cell surface by β-Glc-Y treatment. It is unclear why AGP21 with β-Glc-Y accumulates only in the transversal walls but not all over the cell walls. These results point out AGP21 as a possible link between RH cell fate phenotype and BR responses in root epidermal cells.

Although we screen for abnormal RH cell fate in several AGP-peptide mutants, only AGP21 deficient mutant *agp21*, and to a lower extent, *agp15* (**Figure S4a–b**), exhibited ectopic contiguous RHs at high levels (≈20% and 12%, respectively) (**Figure 2a**). Both *AGP21* expression under its endogenous promoter (*AGP21p::V-AGP21/agp21*) and overexpression (*35Sp::V-AGP21/agp21*) restored a wild type RH phenotype and patterning to *agp21* (**Figure 2a**), confirming that deficient *AGP21* expression causes contiguous RH development. Furthermore, while β-Glc-Y treatment triggered up to ≈35% of contiguous RH (vs. ≈2–5% induced by α-Man-Y) in the wild type (**Figure S1a**), it induced no additional anomalous RH in *agp21* (vs. α-Man-Y treatment or untreated roots) (**Figure 2a**). We tested whether the closely related BZR1-induced peptide AGP15 functions with AGP21 (Sun et al. 2010). *agp15* (**Figure S4c–d**) exhibited a milder phenotype than *agp21*, and the double *agp15 agp21* double mutant had no additional effects to *agp21* (**Figure S4e**). Together, these results confirm that β-Glc-Y might affect *O*-glycosylated AGP21 to stimulate contiguous RH development. The contiguous RH phenotype detected in all genotypes including *agp21* and Yariv-treated roots in this study positively correlates with a higher density of RH in the root epidermis in the same lines in a linear manner ($r^2$= 0.795) (**Fig. S4f**). This confirms that contiguous RH phenotype produces more RHs per epidermis area.

**_O_-glycosylation is required for the correct targeting of the AGP21 peptide to the plasma membrane-apoplastic space**

To determine whether functional AGP21 requires *O*-glycosylation, three putative *O*-glycosylation sites were mutated (Pro→Ala) (**Figure 2b**) and driven by the endogenous *AGP21* promoter in *agp21* (*AGP21p::V-AGP21$^{ALA}$/agp21*). Mass spectrometry had detected that all three proline units (Pro/P) within the AGP21 sequence ATVEAPAPSPTS can be hydroxylated as ATVEAOAOSOTS (Hyp= O) (Schultz et al. 2004), indicating likely sites for *O*-glycosylation. Even though AGP21$^{ALA}$ protein was detected in root epidermal cells (**Figure S5b**), AGP21$^{ALA}$ failed to rescue the *agp21*

RH phenotype (**Figure 2a**). Moreover, β-Glc-Y treatment did not induce anomalous RH cell fate in AGP21$^{ALA}$ plants. Then, we examined whether AGP21 expressed in *Nicotiana benthamiana* colocalized with the BRI1 co-receptor BAK1 (**Figure 2c**). V-AGP21 partially colocalized with BAK1-mRFP protein (**Figure 2c**). When epidermal cells were plasmolyzed, most AGP21 signal localized to the apoplast but some remained close to the PM (**Figure 2c**). V-AGP21$^{ALA}$, however, never reached the cell surface; retention in the secretory pathway could indicate that *O*-glycans direct AGPs to the PM–cell surface (**Figure S5a–b**). These data is in agreement with previous reports of a requirement for *O*-glycans in the secretion and targeting of AGPs and related fasciclin-like AGPs (Xu et al 2008; Xue et al 2017). It is important to note that when AGP21 is transiently overexpressed in *Nicotiana benthamiana,* most of the expression remains in the apoplast and AGP21 is possibly highly O-glycosylated (**Figure 2c and 2e**) while the expression is under the control of its endogenous promoter in *Arabidopsis* most of the signal is linked to the plasma membrane and secretory pathway with less putative *O*-glycosylated isoforms (**Figure 2d, 2e, S1c** and **S5a**). This difference may be linked to both, expression and *O*-glycosylation levels of AGP21. Then, we quantify the expression levels of AGP21p::V-AGP21 in trichoblast and atricoblast cell layers in the root meristematic zone. Although the pattern of AGP21 expression is patchy and irregular, the overall levels of AGP21 are significantly higher in atrichobast cell layers (807±87 Arbitrary Units) than in trichoblast cells (607±31 Arbitrary Units) (**Figure 2d**). This is in agreement with the contiguous RH phenotype shown by the *agp21* mutant suggesting that AGP21 function is related to atrichoblast cell fate.

We tested the hypothesis that AGP21 is processed and modified during its synthesis along the secretory pathway. Using immunoblot analysis, we examined the apparent molecular weight of AGP21 peptide in transient AGP21-overexpressing plants and in *AGP21p::V-AGP21* plants (**Figure 2e**). In the overexpressing plants, most AGP21 peptide was detected as a strong broad band around ≈100–120 kDa with minor bands at ≈80 and ≈55 kDa, whereas endogenously driven AGP21 produced a stronger band at ≈80 kDa and lacked the band at ≈55 kDa, suggesting that, in both cases, AGP21 peptide might be present in a putative tri-*O*-glycosylated form. Mature peptide with no posttranslational modifications is approximately 30 kDa; the extra bands could be interpreted as intermediate single- and di-*O*-glycosylated forms of AGP21 peptide. An

apparent molecular shift of ≈25–30 kDa for each putative *O*-glycosylation site in AGP21 accords with AGP14 peptide, whose protein sequence is highly similar (Ogawa-Ohnishi & Matsubayashi 2015), and with the electrophoretic migration of an AGP-xylogen molecule that contains two arabinogalactan-*O*-Hyp sites (Motose et al. 2004). V-AGP21$^{ALA}$, which lacks *O*-glycans, showed much lower expression, is not targeted to the cell surface, formed puncta-structures (**Figure S5b**) and showed one band close to ~55 kDa (**Figure 2e**) and one band close to ~30 kDa. It is hypothesized here that lack of *O*-glycans in V-AGP21$^{ALA}$ may cause self-interactions and this is compatible with the punctuated structure visualized in the root epidermal cells (**Figure S5b**). A detailed analysis is required to characterize *O*-glycosylation in AGP21 peptide although it is technically challenging due to its carbohydrate complexity. AGP21$^{ALA}$ failure to rescue the *agp21* RH mutant phenotype is possibly due to several reasons, including the lack of Hyp-linked *O*-glycans on its peptide that may affect its function, its lower expression level when compared to *AGP21p::V-AGP21* (**Figure 2d**), and the final cell targeting of the mutated version of AGP21 that differs from the *AGP21p::V-AGP21* functional version (**Figure S5a–b**).

**_O_-glycans stabilize AGP21 peptide's functional conformation**

To address the effect of *O*-glycan on the conformation and stability of AGP21 peptide, we modeled a minimal, 15-sugar Hyp-*O*-linked arabinogalactan (AG) structure ([ATVEAP(O)AP(O)SP(O)TS], **Figure S6a–b**). This is the simplest carbohydrate structure characterized for a single AGP synthetic peptide (Tan et al. 2004), although more complex structures were described for several AGPs (Kitazawa et al. 2013). To assess the conformation of AGP21 peptide and the effect of *O*-glycosylation, molecular dynamics (MD) simulations considered three non-glycosylated peptides (with alanines [nG-Ala], prolines [nG-Pro], or hydroxyprolines residues [nG-Hyp], respectively) and one *O*-glycosylated peptide with three Hyp-*O*-glycans (**Figure S6c**). In the MD simulations, the root mean square deviation (RMSD) varied up to ≈6 Å (**Figure S6d**), indicating that peptide structure may have deviated from the starting type-II polyproline helix. By contrast, larger conformational stabilization effects were observed in the *O*-glycosylated peptide (**Figure S6e**). Individual residue RMSF analysis indicated that the peptide's stiffer region depended on the MD conditions applied (**Figure S6f**). To characterize conformational profiles, we measured the angle formed by four consecutive alpha carbon atoms

(ζ angle) (**Table S3**). The ζ angle of a type-II polyproline helix is –110 ± 15°. In this context, the *O*-glycosylated AOAOSOTS peptide structure is slightly extended between Pro2–Thr7, as observed by ζ angles 2–4 closer to 180° (**Table S3**). Our analysis suggests that *O*-linked glycans affect the conformation and stability of AGP21 peptide. How this conformational change in mature AGP21 peptide without *O*-glycans affects its function in RH cell determination remains unclear and merits further investigation in the future.

**AGP21 acts in a BIN2-dependent pathway to define RH cell fate**

We hypothesized that disrupting AGPs activity with β-Glc-Y, a lack of AGP21 peptide (*agp21*), or abnormal glycosylation on AGP and related proteins, would interfere with BR responsiveness and RH cell fate. We treated the triple mutant *gsk* (*gsk triple*: *bin2-3 bil1 bil2*; BIL1, BIN2-like 1 and BIL2, BIN2-like 2), which almost completely lacks RH cells [1], with 5 µM β-Glc-Y treatment. *Gsk triple* exhibited few contiguous RH cells before and after the treatment (**Figure 3**), suggesting that β-Glc-Y requires BIN2-BIL1-BIL2 to alter RH cell fate. Interestingly, β-Glc-Y induced ≈40-45% contiguous RHs (**Figure 3**) in the constitutively active mutant *bin2-1* (Li & Nam 2002). These data suggest that the AGP-mediated RH cell fate reprogramming requires active BIN2, BIL1, and BIL2 proteins (**Figure 3a**).

As *BRI1* expression is similar in trichoblast and atrichoblast cell layers (Fridman et al., 2014), we sought to determine whether BRI1 and downstream BR responses when AGPs are perturbed, act differently in these cell types during RH cell fate determination (**Figures 3b**). We examined the effect of cell type-specific *BRI1* expression on the percentage of contiguous RHs in three plant lines expressing BRI1-GFP, all in the *bri1-116* background: trichoblast-only (*COBL9p::BRI1-GFP/bri1-116*), atrichoblast-only (*GL2p::BRI1-GFP/bri1-116*), and expression in both cell types (*GL2p::BRI1-GFP* + *COBL9p::BRI1-GFP/bri1-116*) (Hacham et al., 2011; Fridman et al., 2014). BRI1 expression in atrichoblasts did rescued *bri1-116* mutant RH phenotype as well as when BRI1 was expressed in both cell types, being similar to wild type (plants showed very low contiguous RHs). On the contrary, the line that expressed BRI1 in trichoblasts showed higher contiguous RH than Wt Col-0 but lower than *bri1-116* (**Figure 3b**). Additionally, *COBL9p::BRI1/bri1-116* where BRI1 is expressed in trichoblast and missing in atrichoblast cells, it was still sensitive to β-Glc-Y. All the

lines tested with BRI1-GFP exhibited high number of contiguous RHs with this treatment in similar trends than Wt Col-0 (**Figure 3b**). These data implies that BR-BRI1 pathway in atrichoblasts is highly sensitive to promote ectopic RH development under AGP disruption with β-Glc-Y and BR-BRI1 in trichoblast also has an effect under β-Glc-Y. In addition, is important to highlight *bri1-116* mutant high number of contiguous RHs is almost insensitive to β-Glc-Y treatment (**Figure 3b**) suggesting that AGP-perturbation and its responses to trigger contiguous RH is mostly dependent on BRI1.

**Disturbance or absence of AGP21 blocks *GL2* expression**

We then tracked epidermal cell fate and analyzed β-Glc-Y and α-Man-Y's translational effects on several markers: an early RH marker (RHD6p::RHD6-GFP), a downstream transcription factor (RSL4p::RSL4-GFP), a late RH marker (EXP7p::EXP7-NLS-GFP), and two atrichoblast markers for GL2 (GL2p::GFP and GL2p::GL2-GFP) (**Figure 4a–e**). β-Glc-Y, not α-Man-Y, repressed GL2 expression and enhanced RHD6, RSL4 and EXP7 expression in contiguous epidermal cells (**Figure 4a–e**). This corroborates the effects of both β-Glc-Y and deficiencies in the AGP *O*-glycosylation pathway on contiguous epidermis cell development. Then, when we expressed RSL4p::RSL4-GFP in *agp21*, two contiguous epidermis cells showed GFP expression, while this rarely occurred in wild type roots (**Figure 4b**). The transcriptional reporter GL2p::GFP/*agp21* showed discontinuous RH patterning similar to β-Glc-Y treatment (**Figure 4d**). This result implies feedback between the lack of AGP21, GL2 repression, and RHD6-RSL4 and EXP7 positive regulation in contiguous epidermal cell development (**Figure 4f**). Constitutively active *bin2-1* phenocopies *agp21* and β-Glc-Y treatment: it represses GL2 expression in some epidermal cells and enhances EXP7-GFP in contiguous epidermal cells, stimulating contiguous RH development (**Figure 4g–h**). In addition, the overall levels of GL2 expression are much lower in *bin2-1* than in Col-0. To test whether AGP21 (and AGPs in general), affect BR responses, we treated roots with 100 nM BL. Wild type roots exhibited repressed RH development as previously reported (Cheng et al. 2014); *agp21* and three GT mutants (*triple hpgt, ray1* and *galt29A*) defective in AGP *O*-glycosylation (**Table S1**) were unaffected by BL treatment (**Figure S5c**), suggesting that *O*-glycosylated AGP21 (and AGPs) are required for promoting BR responses and downstream signalling on RH cell fate.

**Conclusions**

In root epidermal cells, atrichoblast fate is the default, while environmental as well as endogenous cues like high levels of BRs promotes *GL2* expression in atrichoblasts to repress RH development (Cheng et al. 2014). In the absence of BRs, active P-BIN2 represses *GL2* expression and *RHD6* and *RSL4* expression proceeds, triggering RH development in atrichoblasts and producing contiguous RHs. Perturbed AGPs and the lack of AGP21 peptide at the cell surface stimulate ectopic RH development (in atrichoblast cells that developed as trichoblasts) similar to that observed in BR mutants. BZR1 regulates *AGP21* expression and the *O*-glycosylated cell surface peptide AGP21 modulates RH cell fate. We propose a model, in which the *O*-glycosylated AGP21 peptide and BR responses are both dependent on BIN2 (and BIL1-BIL2)-mediated responses, controlling RH cell fate (**Figure S7**). It is still unclear how the cell surface peptide AGP21 is able to trigger a change in RH cell fate in a BIN2-dependent manner. One possibility is that AGP21 peptide might modify the responsiveness to BRs of the co-receptors BRI1-BAK1. In line with this, we failed to detect a direct interaction between V-AGP21 and BAK1-mRFP in a transient expression system (results not shown). Nonetheless, measuring direct physical interactions between *O*-glycosylated AGP21 and BRI1–BAK1 proteins in the apoplast–PM space is a challenge for a future study. In concordance with this scenario, other GPI anchor proteins (e.g. like LORELEI-like-GPI-anchored protein 2 and 3, LRE/LLG2,3) are able to interact with CrRLK1s (e.g. FERONIA and BUP1,2/ANXUR1,2) in the cell surface of polar growing plant cells (Li et al. 2015; 2016; Lui et al. 2016; Ge et al. 2019; Feng et al.2019). These results imply an interesting parallel between plant AGPs and animal heparin sulfate proteoglycans (HSPGs), which are important co-receptors in signaling pathways mediated by growth factors, including members of Wnt/Wingless, Hedgehog, transforming growth factor-β, and fibroblast growth factor family members (Lin 2004). A second scenario is that AGP21 peptide and BR co-receptors BRI1-BAK1 do not interact in the cell surface and both influence by different pathways BIN2 activity and the downstream RH cell fate program. If this is the case, AGP21 may require other proteins to transduce the signal toward BIN2 in the cytoplasm. Future work should investigate which of these two hypotheses might explain the role of AGP21 peptide in RH cell fate.

**Acknowledgements**

We thank ABRC (Ohio State University) for providing T-DNA lines seed lines. We would like to thank Dr. Sigal Savaldi-Goldstein for providing GL2::BRI1-GFP, COBL9::BRI1-GFP and Gl2::BRI1-GFP + COBL9::BRI1-GFP reporter lines, Dr. Paul Dupree for providing *fut4* and *fut6* mutant lines, Dr. Santiago Mora García for providing *bzr1* and *bes1* mutant lines, Dr. Ana Caño Delgado for providing seeds of BRI1-GFP, *bin2-1* and BZR-YFP, and Dr. Gustavo Gudesblat for providing *gsk triple* mutant seeds. Dr. Malcolm Bennet and Dr. Liam Dolan for the RHD6-GFP and RSL4-GFP lines. This work was supported by grants from ANPCyT (PICT2014-0504, PICT2016-0132 and PICT2017-0066), ICGEB CRP/ARG16-03, and Instituto Milenio iBio – Iniciativa Científica Milenio, MINECON to J.M.E.

**Author Contribution**

C.B, J.G.D and M.M.R performed most of the experiments, analysed the data and wrote the paper. M.C.S analysed the phenotype of glycosyltransferase mutants and BRI1-GFP reporters. L.P.F and H.V. performed molecular dynamics simulations and analysed this data. B.V. analysed the molecular dynamics simulations data. M.C synthesized α-Man-Y and β-Glc-Y reagents. G.S. commented on the project, read the manuscript, and commented on the results. S.M. and E.M. analysed the data and commented on the results. J.M.P., D.R.R.G., Y.d.C.R.G., and S.M.V commented on the results. J.M.E. designed research, supervised the project, and wrote the paper. This manuscript has not been published and is not under consideration for publication elsewhere. All the authors have read the manuscript and have approved this submission.

**References**

Balcerowicz, D., Schoenaers, S. and Vissenberg, K. (2015). Cell fate determination and the switch from diffuse growth to planar polarity in Arabidopsis root epidermal cells. *Front. Plant Sci.* 6, 949

Barnett, N.M. (1970) Dipyridyl-induced Cell Elongation and Inhibition of Cell Wall Hydroxyproline Biosynthesis. *Plant Physiol* 45: 188-191

Berendsen HJC, Postma JPM, van Gunsteren WF, DiNola A, Haak JR (1984) Molecular-dynamics with coupling to an external bath. *The Journal of Chemical Physics* 81:3684-3690

Berendsen HJC, Grigera JR, Straatsma TPJ (1987) The missing term in effective pair potentials. *The Journal of Physical Chemistry* 91:6269-6271

Bussi G, Donadio D, Parrinello MJ (2007) Canonical sampling through velocity rescaling. *The Journal of Chemical Physics* 126:014101

Cheng, Y., Zhu, W., Chen, Y., Ito, S., Asami, T. and Wang, X. (2014). Brassinosteroids control root epidermal cell fate via direct regulation of a MYBbHLH-WD40 complex by GSK3-like kinases. *eLife* 3, e02525

Ding L. and Zhu JK. (1997). A role for arabinogalactan-proteins in root epidermal cell expansion. *Planta* 203:289–94

Feng H., Liu C., Fu R., Zhang M., Li H., Shen L., Wei Q., Sun X., Xu L., Ni B., and Li C. (2019). LORELEI-LIKE GPI-ANCHORED PROTEINS 2/3 regulate pollen tube growth as chaperones and coreceptors for ANXUR/BUPS receptor kinases in *Arabidopsis*. *Mol. Plant.* doi.org/10.1016/j.molp.2019.09.004

Fridman Y, Elkouby L, Holland N, Vragovic K, Elbaum R, Savaldi- Goldstein S. (2014). Root growth is modulated by differential hormonal sensitivity in neighboring cells. Genes Dev. 28:912-920

Ge Z., Zhao Y., Liu M-Ch, Zhou L-Z, Wang, L., Zhong S., Hou, S., Jiang, J., Liu, T., Huang, Q., Xiao, J., Gu, H., Wu H-M, Dong J., Dresselhaus T., Cheung A.Y., Qu L-J. (2019) LLG2/3 are co-receptors in BUPS/ANX-RALF signaling to regulate Arabidopsis pollen tube Integrity. *Current Biology* 29, 1–10

Guan Y, Nothnagel EA (2004) Binding of arabinogalactan proteins by Yariv phenylglycoside triggers wound-like responses in *Arabidopsis* cell cultures. *Plant Physiol* 135:1346–136

Hacham Y, Holland N, Butterfield C, Ubeda-Tomas S, Bennett MJ, Chory J, Savaldi-Goldstein S. (2011). Brassinosteroid perception in the epidermis controls root meristem size. *Development (Cambridge, England)* 138:839–848. doi: 10.1242/dev.061804.

Hess B, Kutzner C, Van Der Spoel D, Lindahl E (2008) GROMACS 4: Algorithms for highly efficient, load- balanced, and scalable molecular simulation. *Journal of Chemical Theory and Computation* 4:435-444

Hess B, Bekker H, Berendsen H.J.C., Fraaije J.G.E.M. (1997) LINCS: A linear constraint solver for molecular simulations. *Journal of Computational Chemistry* 18:1463-1472

Hothorn M, Belkhadir Y, Dreux M, Dabi T, Noel JP, Wilson IA, Chory J. (2011). Structural basis of steroid hormone perception by the receptor kinase BRI1. *Nature* 474:467–471. doi: 10.1038/nature10153

Hutten SJ, Hamers DS, Aan den Toorn M, van Esse W, Nolles A, BuÈcherl CA, de Vries SC, Hohlbein J, Borst JW. (2017) Visualization of BRI1 and SERK3/BAK1 nanoclusters in *Arabidopsis* roots. *PLoS ONE* 12(1): e0169905.doi:10.1371/journal.pone.01699056

Kitazawa K, Tryfona T, Yoshimi Y, Hayashi Y, Kawauchi S, Antonov L, Tanaka H, Takahashi T, Kaneko S, Dupree P, et al. (2013). β-Galactosyl Yariv Reagent Binds to the β-1,3-Galactan of Arabinogalactan Proteins. *Plant Physiology* 161(3): 1117-1126. doi:10.1104/pp.112.211722

Kuppusamy KT, Chen AY, Nemhauser JL. (2009). Steroids are required for epidermal cell fate establishment in Arabidopsis roots. *Proceedings of the National Academy of Sciences of the United States of America* 106: 8073–8076. doi: 10.1073/pnas.0811633106

Li J, Chory J. (1997). A putative leucine-rich repeat receptor kinase involved in brassinosteroid signal transduction. *Cell* 90:929–938. doi: 10.1016/S0092-8674(00)80357-8

Li J, Nam KH (2002) Regulation of brassinosteroid signaling by a GSK3/SHAGGY-like kinase. *Science* 295(5558):1299–1301

Li, C., Wu, H.-M., and Cheung, A.Y. (2016). FERONIA and her pals: functions and mechanisms. *Plant Physiol.* 171, 2379–2392

Li, C., Yeh, F.L., Cheung, A.Y., Duan, Q., Kita, D., Liu, M.C., Maman, J., Luu, E.J., Wu, B.W., Gates, L., et al. (2015). Glycosylphosphatidylinositol anchored proteins as chaperones and co-receptors for FERONIA receptor kinase signaling in Arabidopsis. *eLife* 4, e06587

Liang Y, Basu D, Pattathil S, Xu W.-L., Venetos, A., Martin, SL, Faik A, Hahn MG, Showalter AM. (2013). Biochemical and physiological characterization of fut4 and fut6 mutants defective in arabinogalactan-protein fucosylation in *Arabidopsis*. *J. Exp. Bot.* 64, 5537–5551. doi:10.1093/jxb/ert321

Lin X. (2004). Functions of heparan sulfate proteoglycans in cell signaling during development. *Development* 131 (24): 6009-6021

Lin, Q., Ohashi,Y., Kato,M., Tsuge,T., Gu,H., Qu,L.J., and Aoyama, T. (2015). GLABRA2 directly suppresses basic helix-loop-helix transcription factor genes with diverse functions in root hair development. *Plant Cell* 27: 2894–2906

Liu, X., Castro, C., Wang, Y., Noble, J., Ponvert, N., Bundy, M., Hoel, C., Shpak, E., and Palanivelu, R. (2016). The role of LORELEI in pollen tube reception at the interface of the synergid cell and pollen tube requires the modified eight-cysteine motif and the receptor-like kinase FERONIA. *Plant Cell* 28, 1035–1052

Ma Y, Zeng W, Bacic A, Johnson K (2018). AGPs trough time and space. *Annual Plant Reviews* 1, 1-38

Majamaa K, Gunzler V, Hanauske-Abel HM, Myllyla R, Kivirikko KI (1986) Partial identity of the 2-oxoglutarate and ascorbate binding sites of prolyl 4-hydroxylase. *J Biol Chem* 261: 7819-7823

Masucci JD, Schiefelbein JW. (1994). The *rhd6* mutation of *Arabidopsis thaliana* alters root-hair initiation through an auxin- and ethylene-associated process. *Plant Physiology* 106:1335–1346. doi: 10.1104/pp.106.4.1335

Masucci JD, Schiefelbein JW. (1996). Hormones act downstream of *TTG* and *GL2* to promote root hair outgrowth during epidermis development in the Arabidopsis root. *The Plant Cell* 8:1505–1517. doi: 10.1105/tpc.8.9.1505

Motose H, Sugiyama M, Fukuda H. (2004) A proteoglycan mediates inductive interaction during plant vascular development. *Nature* 429, 873–878

Ogawa-Ohnishi, M., Matsubayashi, Y. (2015). Identification of three potent hydroxyproline O-galactosyltransferases in *Arabidopsis*. *Plant J.* 81, 736–746. doi: 10.1111/tpj.12764

Pereira, A.M., Pereira, L.G., and Coimbra, S. (2015). Arabinogalactan proteins: rising attention from plant biologists. *Plant Reprod.* 28, 1–15

Pol-Fachin L, Verli H (2012) Structural glycobiology of the major allergen of *Artemisia vulgaris* pollen, Art v 1: O-glycosylation influence on the protein dynamics and allergenicity. *Glycobiology* 22:817-825

Ryu KH, Kang YH, Park YH, Hwang I, Schiefelbein J, Lee MM. (2005). The WEREWOLF MYB protein directly regulates *CAPRICE* transcription during cell fate specification in the *Arabidopsis* root epidermis. *Development (Cambridge, England)* 132:4765–4775. doi: 10.1242/dev.02055

Sardar HS, Yang J, Showalter AM (2006) Molecular interactions of arabinogalactan proteins with cortical microtubules and F-actin in Bright Yellow-2 tobacco cultured cells. *Plant Physiol* 142: 1469–1479

Savaldi-Goldstein S, Peto C, Chory J. (2007). The epidermis both drives and restricts plant shoot growth. *Nature* 446:199–202. doi: 10.1038/nature05618

Schiefelbein, J., Huang, L. and Zheng, X. (2014). Regulation of epidermal cell fate in Arabidopsis roots: the importance of multiple feedback loops. *Front. Plant Sci.* 5, 47

Schultz CJ, Ferguson KL, Lahnstein J, Bacic A (2004) Post-translational modifications of arabinogalactan-peptides of *Arabidopsis thaliana*: endoplasmic reticulum and glycosylphosphatidylinositol-anchor signal cleavage sites and hydroxylation of proline. *J Biol Chem* 279: 45503–45511

Seifert, G.J. and Roberts, K. (2007). The biology of arabinogalactan proteins. *Annual Review of Plant Biology* **58**: 137–161

She J, Han Z, Kim TW, Wang J, Cheng W, Chang J, Shi S, Wang J, Yang M, Wang ZY, Chai J. (2011). Structural insight into brassinosteroid perception by BRI1. *Nature* 474:472–476. doi: 10.1038/nature10178

Song SK, Ryu KH, Kang YH, Song JH, Cho YH, Yoo SD, Schiefelbein J, Lee MM. (2011). Cell fate in the Arabidopsis root epidermis is determined by competition between WEREWOLF and CAPRICE. *Plant Physiology* 157:1196– 1208. doi: 10.1104/pp.111.185785

Sun, Y., Fan, X.Y., Cao, D.M., Tang, W., He, K., Zhu, J.Y., He, J.X., Bai, M.Y., Zhu, S., Oh, E., et al. (2010). Integration of brassinosteroid signal transduction with the transcription network for plant growth regulation in Arabidopsis. *Dev. Cell* 19, 765–777

Tan, L., Showalter, A.M., Egelund, J., Hernandez-Sanchez, A., Doblin M.S., and Bacic, A. (2012). Arabinogalactan-proteins and the research challenges for these enigmatic plant cell surface proteoglycans. *Front. Plant Sci.* 3: 140

Tan, L., Qiu, F., Lamport, D.T.A., and Kieliszewski, M.J. (2004). Structure of a hydroxyproline (Hyp)-arabinogalactan polysaccharide from repetitive Ala-Hyp expressed in transgenic *Nicotiana tabacum*. *J. Biol. Chem.* 279: 13156–13165

Tironi IG, Sperb R, Smith PE, van Gunsteren WF (1995) A generalized reaction field method for molecular-dynamics simulations. *The Journal of Chemical Physics* 102:5451-5459

Tryfona, T., Theys, T.E., Wagner,T., Stott,K., Keegstra, K., Dupree, P. (2014). Characterisation of FUT4 and FUT6 α-(1→2)-fucosyltransferases reveals that absence of root arabinogalactan fucosylation increases *Arabidopsis* root growth salt sensitivity. *PLoS ONE* 9:e93291. doi:10.1371/journal.pone.0093291

Van Hengel AJ, Barber C, Roberts K. (2004). The expression patterns of arabinogalactan-protein *AtAGP30* and *GLABRA2* reveal a role for abscisic acid in the early stages of root epidermal patterning. *The Plant Journal: for Cell and Molecular Biology* 39:70–83. doi: 10.1111/j.1365-313X.2004.02104.x.

Velasquez, S.M., Ricardi, M.M., Dorosz, J.G., Fernandez, P.V., Nadra, A.D., Pol-Fachin, L., Egelund, J., Gille, S., Ciancia, M., Verli, H., et al. (2011). O-glycosylated cell wall extensins are essential in root hair growth. *Science* 332:1401–1403

Velasquez, SM, Ricardi MM, Poulsen CP, Oikawa A, Dilokpimol A, Halim A, Mangano S, Denita Juarez SP, Marzol E, Salgado Salter JD et al. (2015a). Complex regulation of prolyl-4-hydroxylases impacts root hair expansion. *Mol Plant.* 8:734–46.

Velasquez, S.M., Marzol, E., Borassi, C., Pol-Fachin, L., Ricardi, M.M., Mangano, S., Denita Juarez SP, Salgado Salter JD, Gloazzo Dorosz J, Marcus SE et al. (2015b). Low sugar is not always good: Impact of specific O-glycan defects on tip growth in *Arabidopsis*. *Plant Physiol.* 168, 808–813.doi: 10.1104/pp.114.255521

Wang L, Li H, Lv X, Chen T, Li R, Xue Y, Jiang J, Jin B, Baluška F, Šamaj J, et al. (2015) Spatiotemporal Dynamics of the BRI1 Receptor and its Regulation by Membrane Microdomains in Living Arabidopsis Cells. *Mol. Plant.* 8(9):1334-1349

Willats W.G. and Knox, J.P. (1996). A role for arabinogalactan-proteins in plant cell expansion: evidence from studies on the interaction of β-glucosyl Yariv reagent with seedlings of *Arabidopsis thaliana*. *Plant J*. 9:919–25

Xu, J., Tan, L., Lamport, D.T.A., Showalter, A.M., and Kieliszewski, M.J. (2008). The O-Hyp glycosylation code in tobacco and Arabidopsis and a proposed role of Hyp-glycans in secretion. *Phytochemistry* 69: 1631–1640

Xue H., Veit, C., Abas, L., Tryfona, T., Maresch, D., Ricardi, M.M., Estevez, J.M., Strasser R., Seifert G.J. (2017). *Arabidopsis thaliana FLA4* functions as a glycan-stabilized soluble factor via its carboxy proximal Fasciclin 1 domain. *Plant J*. 10.1111/tpj.13591

Yan Z, Zhao J, Peng P, Chihara RK, Li J. (2009). BIN2 functions redundantly with other Arabidopsis GSK3-like kinases to regulate brassinosteroid signaling. *Plant Physiology* 150:710–721. doi: 10.1104/pp.109.138099

Yang CJ, Zhang C, Lu YN, Jin JQ, Wang XL. (2011). The mechanisms of brassinosteroids' action: from signal transduction to plant development. *Mol. Plant* 4:588–600. doi: 10.1093/mp/ssr020

Yariv J, Lis H, Katchalski E (1967) Precipitation of arabic acid and some seed polysaccharides by glycosylphenylazo dyes. *Biochem J* 105(1):1C–2C

Yi, K., Menand, B., Bell, E., and Dolan, L. (2010). A basic helix-loop-helix transcription factor controls cell growth and size in root hairs. *Nat. Genet.* 42, 264–267. doi: 10.1038/ng.529

Zavaliev R., Dong, X., Epel B.L. (2016) Glycosylphosphatidylinositol (GPI) modification serves as a primary plasmodesmal targeting signal. *Plant Physiology*. 172(2): 1061-1073

**Supporting Information**

The following Supporting Information is available for this article:

**Figure 1. Contiguous root hair (RH) phenotype in *O*-underglycosylated arabinogalactan proteins (AGPs) phenocopy brassinosteroid (BR) mutants in *Arabidopsis thaliana*.**

(**a**) RH phenotype in three glycosyltransferase (GT) mutants (*triple hpgt*, *ray1*, *galt29A* and *fut4 fut6*) that act specifically on AGP *O*-glycosylation. Effect on contiguous RH phenotype in roots treated with 5µM α-Mannosyl Yariv (α-Man-Y) or 5µM β-Glucosyl Yariv (β-Glc-Y).

(**b**) RH phenotype in the *p4h5* mutant and in four glycosyltransferase mutants (*triple hpgt*, *ray1*, *galt29A*, and *fut4 fut6*) that act specifically on AGP *O*-glycosylation. Right, selected pictures. Arrowheads indicated two contiguous RHs. Scale bar= 50 µm.

(**c**) The mutants used in (B) for the GTs involved in AGP *O*-glycosylation are indicated.

(d) RH phenotype in two glycosyltransferase mutants (*rra3* and *rra3 sgt1*) that act specifically on EXT *O*-glycosylation. Effect on contiguous RH phenotype in roots treated with 5µM α-Mannosyl Yariv (α-Man-Y) or β-Glucosyl Yariv (β-Glc-Y).

(**e**) The mutants used in (d) for the GTs involved in EXT *O*-glycosylation are indicated.

(a, b and d) *P*-value of one-way ANOVA, (**) $P<0.001$, (*) $P<0.01$. NS= not significant different. Error bars indicate ±SD from biological replicates.

See also Figure S1-S4.

**Figure 2. *O*-glycosylated AGP21 peptide at the cell surface modulates root hair (RH) cell fate in *Arabidopsis thaliana*.**

(**a**) Contiguous RH phenotype in *agp21*, complemented *agp21* mutant with AGP21::V-AGP21 and with 35S::V-AGP21 constructs as well as AGP21::V-AGP21$^{ALA}$ expression in *agp21*. Only one line is shown. *P*-value of one-way ANOVA, (***) $P<0.001$. NS= not significant differences. Error bars indicate ±SD from biological replicates.

(**b**) Identified AGP21 peptide acting on root epidermis development. AGP21 peptide sequence and its posttranslational modifications carried out in the secretory pathway. The mature AGP21 peptide contains only 10-13 aa in length. APO= Apoplast. ER=Endoplasmic Reticulum. GPI anchor= GlycosylPhosphatidylInositol (GPI) anchor. PM=Plasma membrane.

(**c**) Co-localization of AGP21-Venus with BAK1-mRFP at the plasma membrane of epidermal cells in *Nicothiana benthamiana*. Scale bar= 10 µm. Cross section of expression levels across BAK1-RFP

coexpressed with AGP21-Venus. On the left, plasmolysis was induced with 800 mM Mannitol uncovering an apoplastic plus plasma membrane AGP21 localization. Arrowheads indicate plasma membrane located AGP21. Scale bar= 10 µm.

(**d**) Expression levels of AGP21-V (AGP21::V-AGP21/*agp21*) in atrichoblast (AT) and trichoblast (T) cell layers of the root meristematic zone. Scale bar= 10 µm.

(**e**) Immunoblot analysis of two stable lines expressing 35S::V-AGP21 (L1-L2) and two lines expressing AGP21::V-AGP21 (L1-L2) and two lines expressing AGP21::V-AGP21$^{ALA}$ (L1-L2). Each blot is an independent experiment. Putative Venus-AGP21 structures are indicated on the right based on the apparent molecular weight. *O*-glycans are indicated as red elongated balloons. ΔOH = non-hydroxylated. ΔGly = without *O*-glycans. 1-Gly to 3-Gly = 1 to 3 sites with Hyp-*O*-glycosylation. Asterisk indicates missing AGP21 glycoforms or lack of Venus protein.

See also Figure S4-S6.

**Figure 3. Perturbation of arabinogalactan proteins (AGPs) requires active BRI1 expression in atrichoblast cells and downstream BIN2-BIL1-BIL2 proteins to triggers changes in root hair (RH) cell fate in *Arabidopsis thaliana*.**

(**a**) Contiguous RH phenotype in roots treated with 5µM β-Glucosyl Yariv (β-Glc-Y) or 5µM α-Mannosyl Yariv (α-Man-Y). Scale bar= 20 µm. *P*-value of one-way ANOVA, (***) $P<0.001$, (*) $P<0.05$. NS= not significant differences. Error bars indicate ±SD from biological replicates. Arrowheads indicated two contiguous RHs. *bin2-1* is a constitutively active mutant of BIN2. *gsk triple* comprises *bin2-3 bil1 bil2* (BIN-2, BIL1 for BIN2-like 1 and BIL2 for BIN2-like 2).

(**b**) Effect of the BRI1 differential expression on the development of contiguous RH. BRI1 is active when expressed in atrichoblast cells (under GL2 promoter).

See also Figure S5.

**Figure 4. Arabinogalactan proteins (AGPs) disruption, the lack of AGP21, and *bin2-1* block the root hair (RH) repressor GLABRA2 (GL2) and triggers RHD6-RSL4-EXP7 expression in some atrichoblast cells in *Arabidopsis thaliana*.**

The effect of β-Glucosyl Yariv (β-Glc-Y), α-Mannosyl Yariv (α-Man-Y), and the absence of AGP21 peptide were monitored on several markers to study epidermis cell fate.

(**a**) RHD6 (RHD6::RHD6-GFP) as an early RH marker.

(**b**) A downstream RHD6 factor RSL4 (RSL4::RSL4-GFP).

(**c**) The RSL4-gene target EXP7 (EXP7::EXP7-NLS-GFP).

(**d**) The main RH repressor GL2 as a transcriptional marker (GL2::GFP).

(**e**) The main RH repressor GL2 as a translational marker (GL2::GL2-GFP).

(**f**) Proposed sequence of events triggered by β-Glucosyl Yariv (β-Glc-Y) or the lack of AGP21 peptide that leads to abnormal RH development.

(**g**) GL2 expression (GL2::GL2-GFP) in the *bin2-1* background in the Meristematic Zone (MZ) and Elongation Zone (EZ) of the root.

(**h**) The RH marker EXP7 expression (EXP7::EXP7-NLS-GFP) in the *bin2-1* background in the Elongation Zone (EZ) of the root.

(**a**-**e** and **g**-**h**) Arrowheads indicate expression of a given marker in two contiguous epidermal cell lines. Asterisks indicated absence of expression. Scale bar= 20 μm.

(**i**) Proposed sequence of events triggered by *bin2-1* that leads to abnormal RH development.

See also Figure S7.

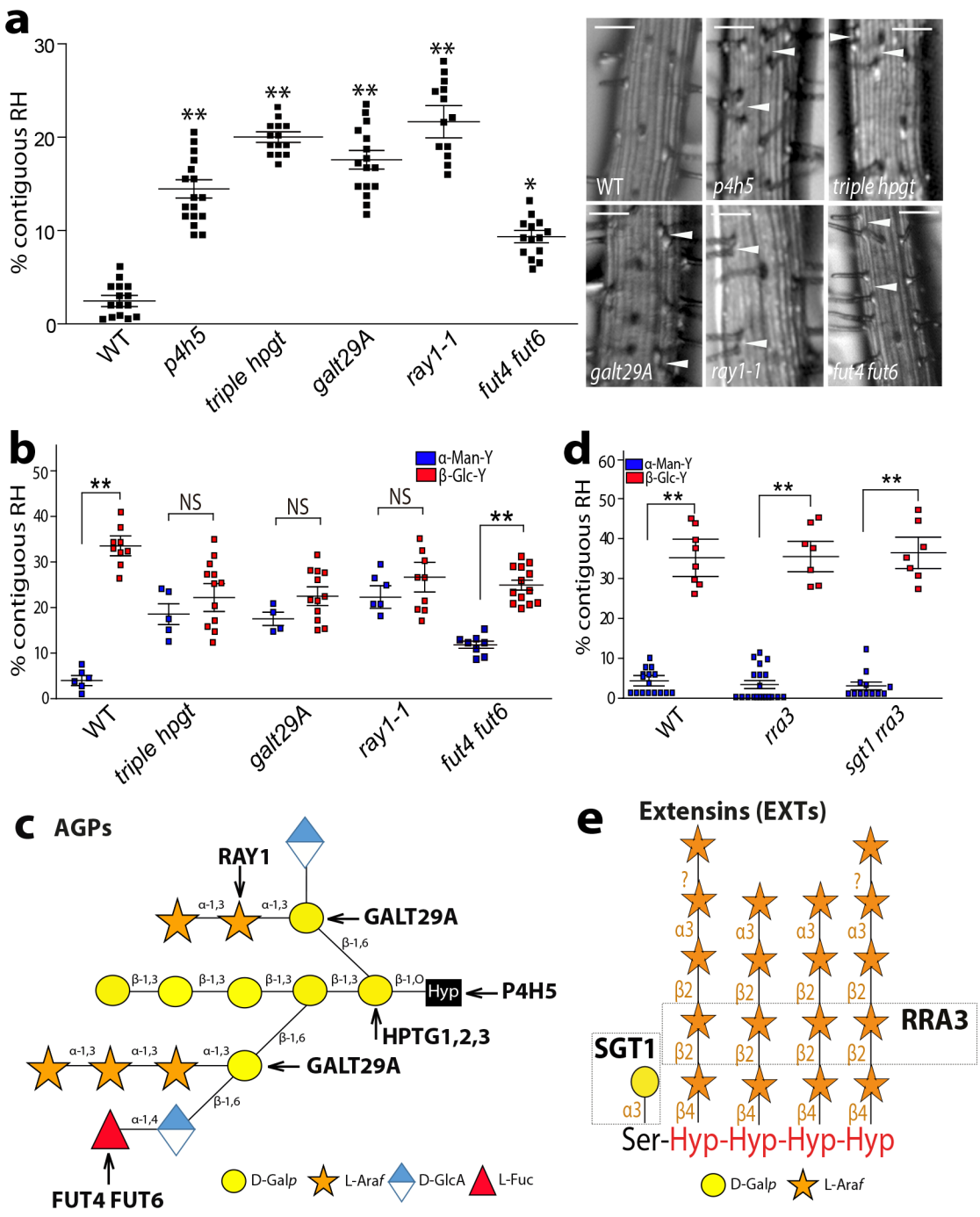


nph_16487_f1.tif

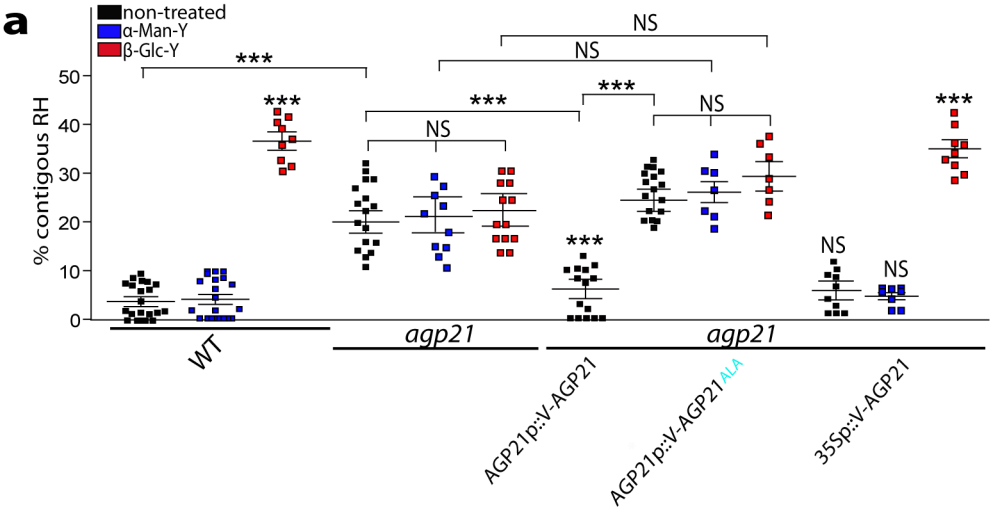


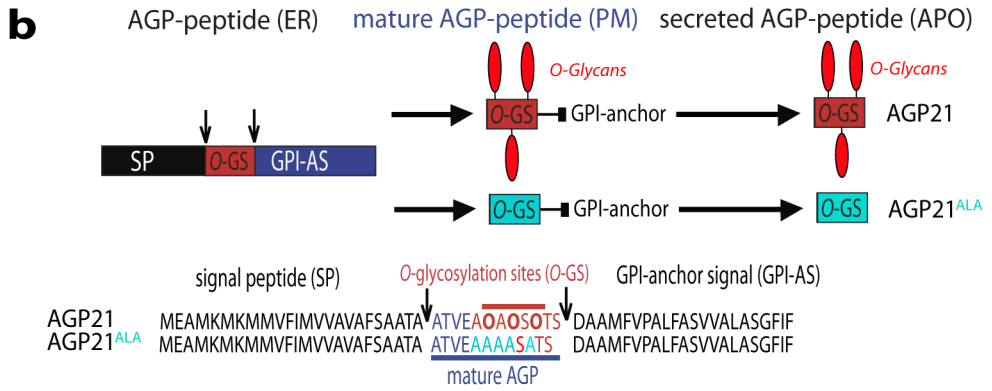


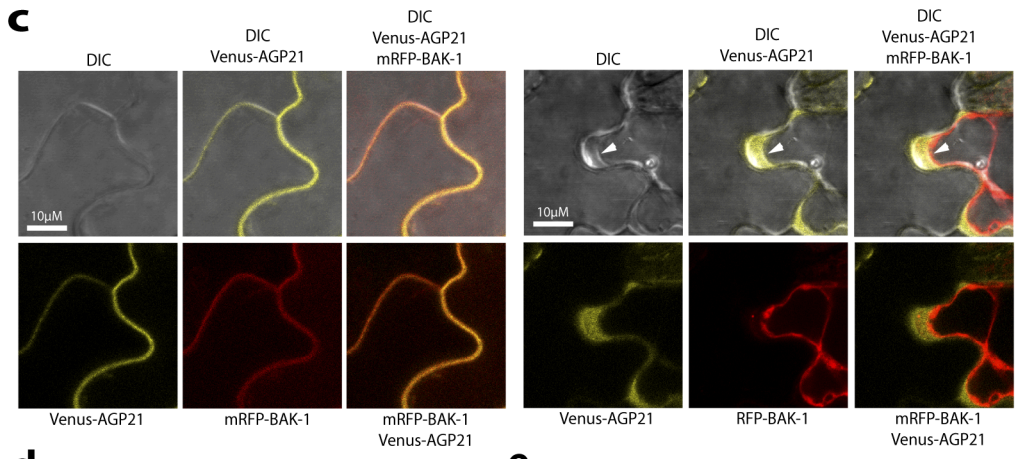


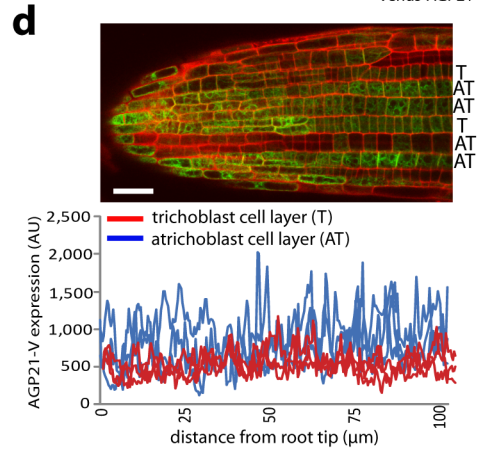


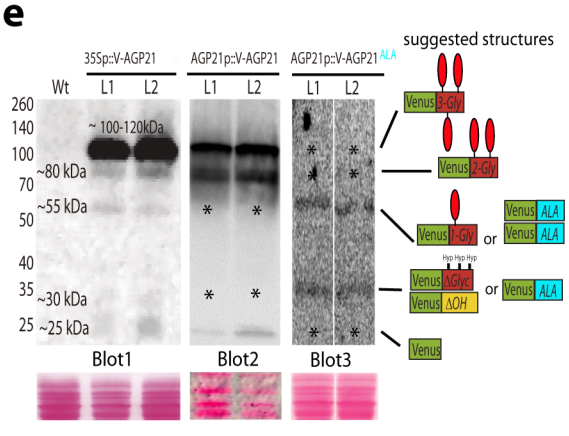

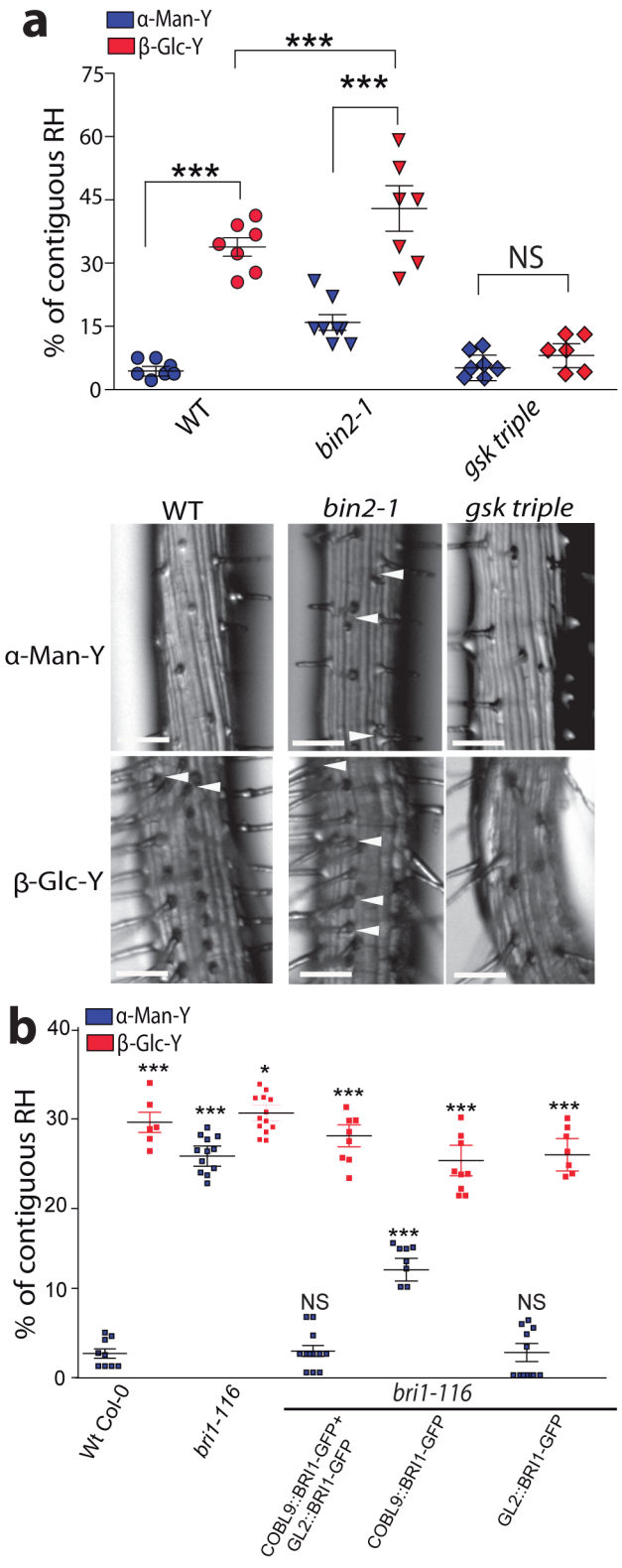


nph_16487_f3.tif

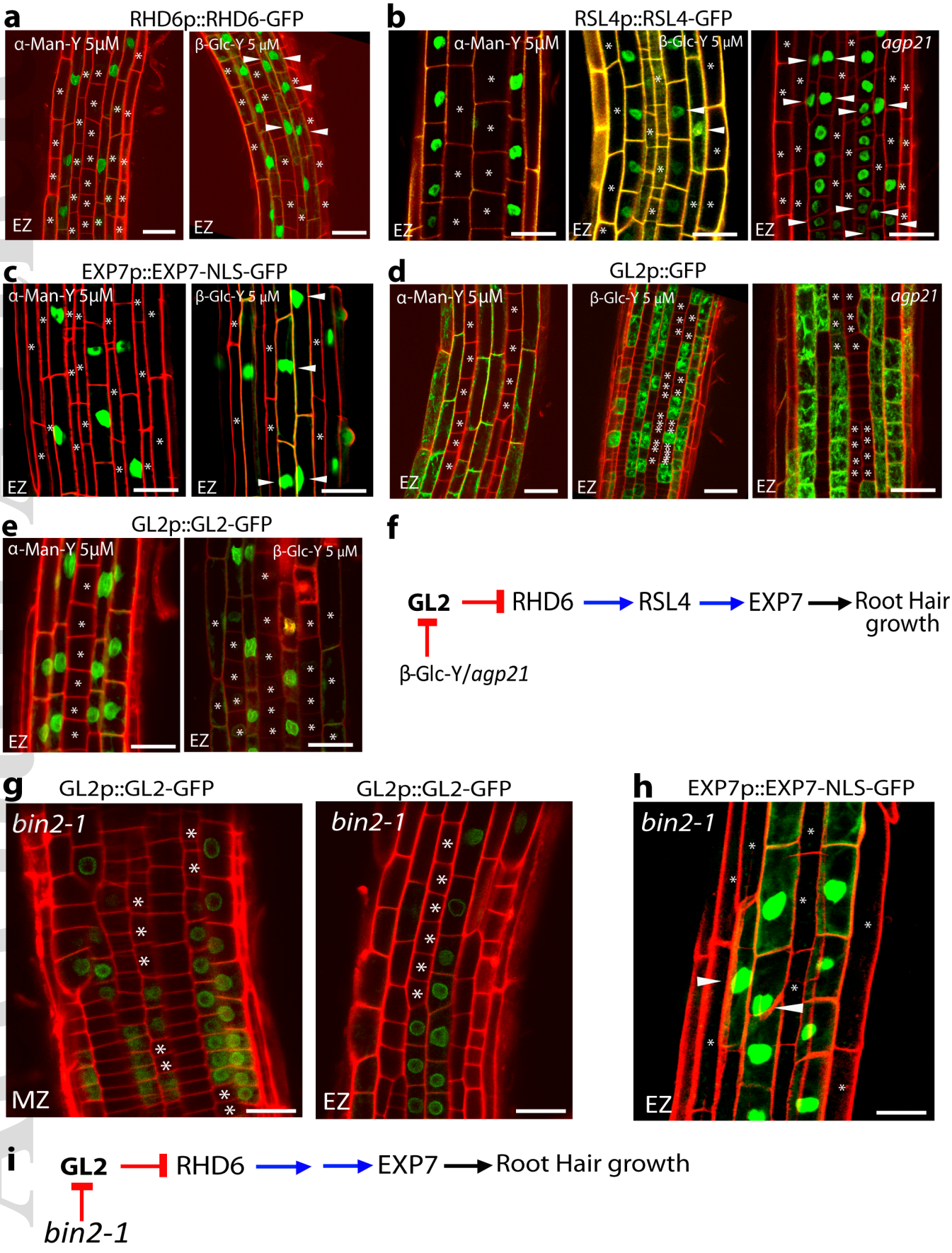


nph_16487_f4.tif